

**Research Article** 

# Self-doped porous carbon derived from acacia plantation residues for green-supercapacitor in sustainable energy applications



Apriwandi<sup>1,\*</sup> D, Rindhu Nabila Deniza<sup>1</sup>, Awaludin Martin<sup>2</sup>, Julnaidi Julnaidi<sup>3</sup>, Rika Taslim<sup>4</sup>, Erman Taer<sup>1</sup>

**ABSTRACT:** To improve bio-organic-carbon quality for supercapacitors, consider using dual or more heteroatom for more profitable carbon-chain doping. Developing suitable sources and preparation strategies is challenging but essential. Herein, we introduce a potential carbon source derived from acacia plantation residues, doped with boron, oxygen, and phosphorus. The pore structure of this carbon material can be precisely tuned to exhibit a well-defined hierarchical arrangement of micro-, meso-, and macropores through a low-ratio of phosphoric acid (H<sub>3</sub>PO<sub>4</sub>) impregnation method combined with dual-environment (N<sub>2</sub> and CO<sub>2</sub>) vertical pyrolysis in one step integrated. The resulting material displays a confirmed hierarchical morphology with a hierarchical transformation into tunnel pores, in specific surface area of 521.70 m<sup>2</sup>/g which contributed to high charge storage and deliverability. Additionally, the material contains significant levels of boron (0.93%), oxygen (9.19%), and phosphorus (0.34%), facilitating a reversible Faradic reaction in the working electrode. Consequently, optimized-electrode achieves a specific capacitance of 198 F/g at 1 A/g in H<sub>2</sub>SO<sub>4</sub> electrolyte. In a two-electrode system, records energy density of 14 Wh/kg (1 A/g) at a maximum power density of 670 W/kg (10 A/g). These findings suggest that the natural incorporation of boron, oxygen, and phosphorus enhances both the activity and the hierarchical pore structure of carbon derived from acacia plantation residues.

**Keywords:** Self-doped, Carbon material, Nano-structure, Electrode material, Supercapacitor

## 1. INTRODUCTION

Acacia plantations are an essential economic resource for Indonesia, and their development has seen significant growth in recent years. In 2022, the total area of acacia plantations (including eucalyptus) reached 2.63 million hectares in Indonesia, primarily concentrated on the islands of Sumatra and Kalimantan. This marked a nearly 30% increase from the 2015 recorded area of around 2.5 million hectares. This rapid growth is due to the rising demand for wood, particularly in the pulp and paper industry. The conversion of nearly 98% of forests to acacia plantations in Kalimantan in 2022 has led to significant amounts of plantation residues, such as dry leaves and acacia pods. However, specific data on the amount of residue produced is limited. Traditionally, most of these residues are treated through conventional burning, which can result in air pollution. Studies have shown that acacia pods, in particular, have a high protein content and contain valuable chemicals such as tannins and phenolic compounds, which have potential biological activity. At the plantation scale, the entire acacia biomass, including pods, plays a significant role in nutrient recycling, especially if residue management is effectively implemented. However, due to the perceived low application rate, conventional burning remains a common option. Despite this, the high protein content, unique and valuable phenolic and tannin chemical compounds, and the presence of abundant nutrients make acacia pods an excellent porous carbon source for energy storage applications, notably supercapacitors.

#### **OPEN ACCESS**

#### **Affiliation**

<sup>1</sup>Department of Physics, Faculty of Mathematic and Natural Science, University of Riau, Pekanbaru 28293, Indonesia.

<sup>2</sup>Department of Mechanical Engineering, Faculty of Engineering, University of Riau, Pekanbaru 28293, Indonesia.

<sup>3</sup>Department of Mechanical Engineering, Sekolah Tinggi Teknologi Pekanbaru 28293, Indonesia.

<sup>4</sup>Department of Industrial Engineering, Faculty of Science and Technology, Universitas Islam Negeri Sultan Syarif Kasim Riau, Pekanbaru 28293, Indonesia.

#### \*Correspondence

Email: apriwandi@lecturer.unri.ac.id

ORCID 📵

Apriwandi: 0000-0003-3560-5571 Rika Taslim: 0000-0003-1946-1299

Received: June 11, 2025 Revised: June 23, 2025 Accepted: Juli 04, 2025

**How to cite:** Apriwandi, Deniza, R., N., Martin, A., Julnaidi, J., Taslim, R., Taer, E., (2025). Self-doped porous carbon derived from acacia plantation residues for green-supercapacitor in sustainable energy applications. *Journal of Applied Materials and Technology*, 7(1), 1–10. https://doi.org/10.31258/Jamt.7.1.1-10.

This article is licensed under a Creative Commons Attribution 4.0 International License.



Recent studies have shown that using plantation residue biomass as a source of porous carbon for supercapacitor applications is very promising [1,2]. This is due to biomass offers various attractive characteristics as a carbon source, such as an easily increased surface area [3,4], an abundant nanoporous structure of rich bio-organic compounds [5,6], confirmed self-doping species [7,8], and easier and environmentally benign production stages [9,10]. For instance, acacia leaves from acacia plantation residues have been transformed into porous nanocarbon with abundant hollow nanofiber morphology for supercapacitor energy storage devices using a relatively simple high-temperature pyrolysis method.

The capacitive properties were found to be 113 F/g at 1 mV/s[11]. In another study, Wang et al., 2024 synthesized hierarchical porous carbon rich in oxygen doping derived from trachycarpus fortune plantation residues through a KOH activation strategy [12]. The surface area detected reached 2049 m<sup>2</sup>/g containing 22.54% oxygen doping. The energy output of the supercapacitor produced was 14.67 Wh/kg with an output power of 320 W/kg. Walnut shell, a walnut plantation residue, was used as a source of nitrogen and sulphur doped carbon by Anand et al., 2024 due to its unique protein content and abundant nutrients [13]. From this carbon material, they obtained a high-performance supercapacitor with a high gravimetric capacitance of 271.4 F/g and a volumetric capacitance of 74.53 F/cm³ at 0.5 A/g. Similar findings were also observed in several other plantation residues such as Sargassum thunbergia [14], Jack wood [15], and rapeseed stalk [16]. These studies indicate that the high protein, abundant chemical compounds, and lignocellulosic content contained in plantation residue biomass are ideal for the development of sustainable green supercapacitor energy storage devices. However, the potential of acacia pods as a carbon source for working electrodes in supercapacitors has not been extensively studied.

In this study, we prepared heteroatom-self-doped porous carbon from acacia pods biomass derivatives using a novel and environmentally friendly approach for green supercapacitor applications. We used an integrated one-step chemical-physical activation method for the synthesis of porous carbon because it is cost-effective and time-efficient.  $\rm H_3PO_4$  solution was chosen as the chemical activating agent, while carbon dioxide was used as the physical activating agent. Additionally, we designed the carbon precursor to be solid without an external binder to maintain high material conductivity. The resulting porous carbon exhibited a hexagonal hierarchical structured morphology with a total surface area of 521.70 m²/g. The ratio of micropores to mesopores was optimized to be 4/1.

Notably, the as-prepared carbon contained abundant heteroatom doping species of phosphorus, boron, and oxygen, which synergized to generate faraday redox reactions in the material. The electrochemical properties of the symmetric supercapacitor were thoroughly studied on both gravimetric and volumetric scales, yielding capacitive values of 198 F/g and 203.4 F/cm³ at 1A/g, respectively. Furthermore, the energy output reached as high as 14 Wh/kg at a maximum power of 670 Wh/kg. Thus, our findings suggest that acacia plantation residues, particularly acacia pods, hold great promise as a self-doped porous carbon source for sustainable next-generation supercapacitor applications.

### 2. EXPERIMENTAL

**2.1. Materials.** The acacia plantation residues refer to acacia pods from community plantations in Pelalawan Regency, Riau, Indonesia, which have not been used. Phosphoric acid (H<sub>3</sub>PO<sub>4</sub>) was selected as the chemical catalyst, supplied by Merck KGaA 1.00573.2500. Nitrogen and carbon dioxide gases were procured from CV. Bintang Sinar Gasindo, an authorized distributor of PT. Samator Indonesia Tbk. Sulfuric acid (H<sub>2</sub>SO<sub>4</sub>, 98%) was provided by Panreac Química S.A.U.

2.2. Preparation of self-doped heteroatom porous carbon. The preparation of self-doped porous carbon followed a series of measurable, systematic, and environmentally benign steps. The material was synthesized using a time-efficient, one-step chemical-physical activation process, leveraging the rich heteroatoms present in the selected biomass. First, the precursor waste was cleaned with distilled water and diced. The water content was removed by drying in an airtight oven at 100°C. The dried precursor was then crushed through grinding, milling, and sieving, with the powder passing through a 250-mesh sieve being collected for further processing. The sieved powder was impregnated with  $H_3PO_4$  at a relatively low concentration (500 mmol/g) using a solvent-to-H<sub>3</sub>PO<sub>4</sub> ratio of 5:1. The mixture was stirred at 80°C for 3 hours using a hotplate stirrer. After stirring, the mixture was dried and ground, ensuring no agglomeration, before being formed into thin cylindrical solids using a manual hydraulic press without external binders. A total of 40 cylindrical pieces were prepared for pyrolysis in a vertical tube furnace.

The pyrolysis process involved one-step integrated: carbonization at  $600^{\circ}$ C under an  $N_2$  atmosphere, followed by physical activation at  $850^{\circ}$ C under  $CO_2$ . The process concluded with cooling under an  $N_2$  atmosphere. The resulting product was washed in distilled water until neutral, yielding a self-doped porous carbon material in a solid-binder-free cylindrical form. The preparation scheme for this doped porous carbon is illustrated in Figure 1.

2.3. Material characterizations. The obtained porous carbons were initially evaluated based on physical shape changes from their solid cylindrical form. This evaluation was carried out by calculating the precursor densities using the density equation, where the mass of each precursor was divided by its geometric volume. Microcrystalline phase shifts were analysed via X-ray diffraction (XRD) in a scan range of 10.0–79.9°, using continuous scan mode, with a scan speed of 2.00°/min and a sampling pitch of 0.0189°. Surface morphology was observed using scanning electron microscopy (SEM) at SED 15.0 kV, WD 10.00 mm, Std-PC 40.0, in high vacuum at a magnification of 10,000x. Elemental composition was determined by energy dispersive spectroscopy (EDS) at 0-20keV. Additionally, the porosity properties, including micro- to mesopore ratios and average pore size distribution, were assessed through nitrogen adsorption analysis, utilizing BET, BJH, DFT, and T-plot methods.

**2.4. Preparation of symmetric supercapacitor cells.** The supercapacitor cells were assembled using a two-electrode symmetric configuration without the use of external adhesives. Two solid carbon cylinders, each with dimensions of 0.2 mm in thickness and 8.0 mm in diameter, were stacked with a thin eggshell membrane separator between them [17]. A 1 M  $\rm H_2SO_4$  solution served as the electrolyte, injected between the electrodes. Stain-

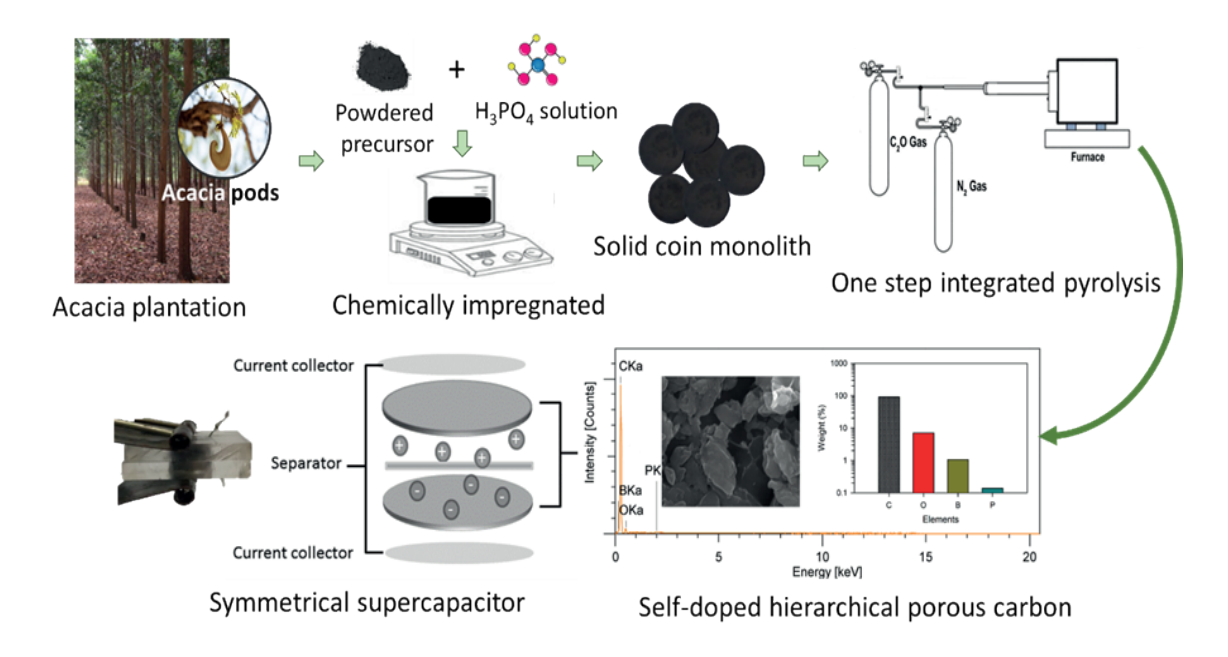


Figure 1. Schematic representation of doped porous carbon produced from acacia plantation residues (acacia pods).

less steel current collectors were positioned on the outer sides of the carbon electrodes, supported by an acrylic cell body to ensure structural integrity.

**2.5. Electrochemical properties measurement.** The electrochemical properties of the symmetric supercapacitors were thoroughly analyzed using cyclic voltammetry (CV) and galvanostatic charge-discharge (GCD) measurements. CV measurements were conducted at a maximum operating voltage of 1 V across various scan rates, with capacitive properties calculated using a previously established equation. Similarly, GCD measurements were performed under the same voltage conditions as the CV tests, but at varying current densities. The specific capacitance, energy density, and power output were calculated using standard formulas commonly applied to symmetric supercapacitor cells [18,19].

# 3. RESULT AND DISCUSSION

Physical changes of the precursor prepared in the form of a thin cylinder are an initial evaluation to ensure the presence of porosity in the carbon material. This assessment is based on changes in precursor density during the pyrolysis process, which integrates carbonization and physical activation in a single stage [20]. Prior to pyrolysis, the thickness, diameter, and mass of the precursor were measured with precision to calculate its density. The same measurements were repeated after pyrolysis. Notably, the high-temperature pyrolysis process resulted in a significant reduction in precursor density, as shown in Figure 2a. Before pyrolysis, the precursor exhibited a density of 0.79 g/cm<sup>3</sup> with a fluctuation range of ±0.04. Upon completion of pyrolysis, the density dropped by approximately 35% to 0.53 g/cm<sup>3</sup>, with a fluctuation of  $\pm 0.05$ . This substantial decrease in density suggests the formation of empty cavities within the precursor, indicating the development of porosity. The porosity arises as a result of various treatments applied during pyrolysis.

During carbonization, conducted at 600°C, volatile components are fully evaporated, and the decomposition of complex compounds such as lignin, hemicellulose, and cellulose occurs, yielding a higher concentration of pure carbon [21,22]. This process also produces tar as a residue, which becomes embedded in the material. Simultaneously, the chemical interaction between H<sub>3</sub>PO<sub>4</sub> and carbon initiates at 600°C, breaking carbon chains and facilitating the formation of pores in the material [23,24]. Physical activation, carried out between 600°C and 850°C, further removes the tar residue from carbonization and expands the existing cavities. This combination of processes results in a drastic reduction in the density of the solid cylindrical precursor, as depicted in Figure 2a. These findings provide early evidence of high porosity in the resulting product, which is advantageous for its application as an electrode material in supercapacitor energy storage systems.

The phase and microcrystalline structures of the as-prepared carbon materials were analysed using X-ray diffraction (XRD), as shown in Figure 2b. The XRD patterns exhibit two broad peaks within the angular ranges of 23.4° and 43.7°, corresponding to the [002] and [100] reflection planes, identified turbostratic carbon to high amorphous structure (JCPDS No. 01-089-7213, 01-089-8493, and 00-046-0943). The broad peak observed at the [002] reflection indicates that the carbon material possesses a layered amorphous structure.

In contrast, the weak broad peak at the [100] reflection suggests a low degree of graphitization, likely due to the catalytic effect of  $\rm H_3PO_4$ , which causes extensive surface modification and disrupts the graphitic structure, leading to a decrease in peak intensity. No additional peaks were observed, confirming the high purity of the carbon material. Moreover, a significant modulation in d-spacing was detected, particularly in the [002] reflection. The d-spacing at [002] was recorded at 0.3987 nm, approximately 11.5% larger than that of conventional graphite, further confirming the material's amorphous structure with an abundance of pores [25]. This

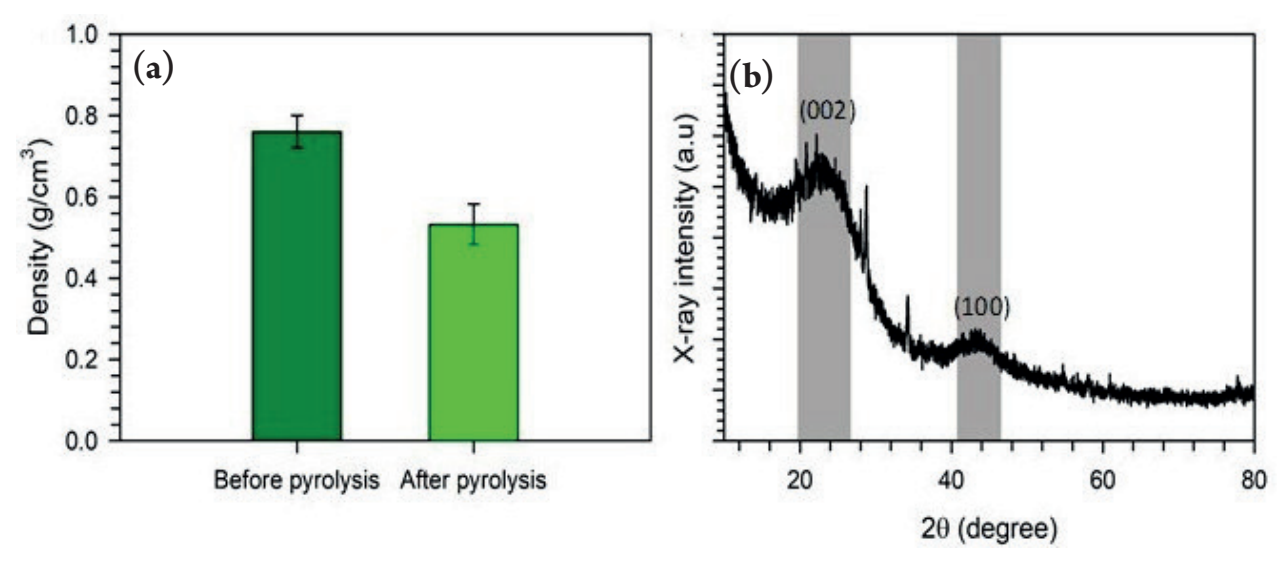


**Figure 2**. (a) Density of porous carbon in pyrolysis process, and (b) XRD pattern of porous carbon.

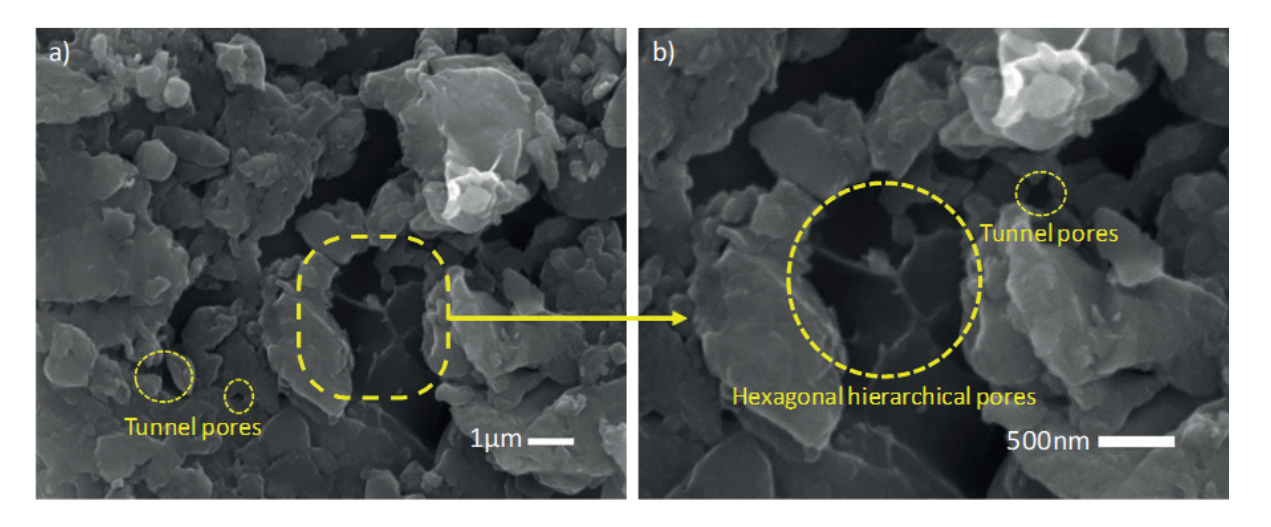


Figure 3. Image SEM of porous carbon in (a)1 μm, and (b) 500 nm

increase in d-spacing also influences the microcrystalline dimension, Lc, where a larger Lc layer height suggests the potential for a high surface area, consistent with empirical formulas reported previously [26]. Additionally, the d-spacing at the [100] reflection was recorded at 0.2033 nm, which is typical for biomass-derived activated carbon materials. These observations point to the material's favourable microstructure, with a combination of amorphous characteristics and high porosity, making it suitable for applications requiring a large surface area.

The surface morphology structure of the acacia reside plantation-derived porous carbon were studied using scanning electron microscopy (SEM), as shown in Figure 3. The one-step integrated chemical-physical activation using  $\rm H_3PO_4$  and  $\rm CO_2$  resulted in a surface morphology characterized by agglomerates and carbon blocks of varying sizes, ranging from the nanoscale to the micrometer scale. Figure 3a displays carbon blocks with sizes between 653nm and 3.1µm, with relatively smooth surfaces, suggesting the predominant formation of micropores within the material. This ob-

servation aligns with previous reports indicating that carbon materials chemically activated at high temperatures typically exhibit surfaces rich in micropores [27,28]. Further confirmation of this microporous structure was obtained through N2 adsorption-desorption analysis, likely due to the etching effect of H<sub>3</sub>PO<sub>4</sub> on the precursor surface. Additionally, higher magnification in Figure 3b reveals a hierarchically interconnected hexagonal pore framework on the precursor surface. This structure plays a crucial role in enhancing the performance of the material as a working electrode for energy storage devices [29]. The physical activation process using CO<sub>2</sub> effectively etched the carbon chains and expanded the pores, leading to the development of mesopores and macropores. This pore expansion creates synergistic effects by providing rapid ion diffusion pathways and ion buffering capacities, which are essential for the improved performance of modern energy storage systems [30].

The porosity characteristics, specific surface area, and pore size distribution of the synthesized carbon were thoroughly analysed

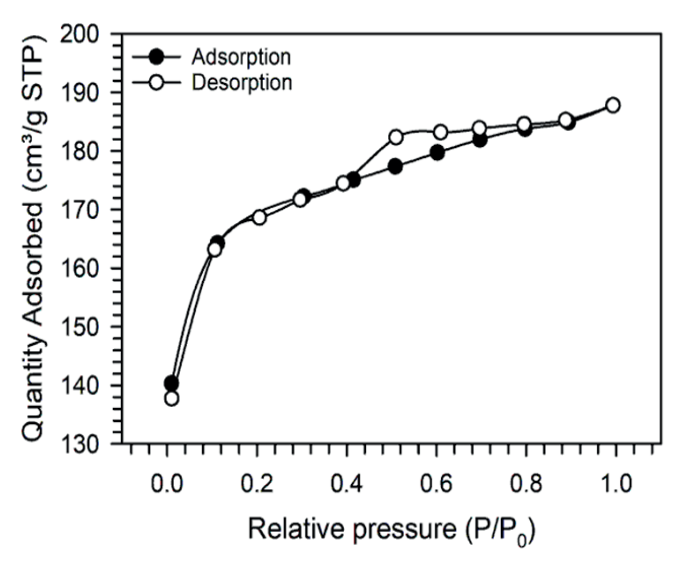


**Figure 4**. N<sub>2</sub> gas adsorption-desorption profile of porous carbon.

using the  $\rm N_2$  adsorption-desorption isotherm method at 77 K. The  $\rm N_2$  isotherm profiles, presented in Figure 4, exhibited a combination of Type I and Type IV adsorption curves, indicative of the coexistence of micropores and mesopores within the material. [31] A significant increase in adsorption at relative pressures of <0.15 suggests the dominant presence of micropores (0-2 nm scale).

Meanwhile, the hysteresis loop observed at relative pressures 0.35-0.90 corresponds to the formation of well-defined mesopores, which are characterized by optimal cylindrical shape [32]. In addition, the slight increase in adsorption at relative 0.95-1.0 is associated with the typical formation of macropores [33]. Using the Braeuer-Emmett-Teller (BET) method, the specific surface area of the carbon was determined to be 521 m<sup>2</sup>/g, with a total pore volume of 0.293 cm<sup>3</sup>/g. Notably, micropores accounted for 80.65% (420.76 m<sup>2</sup>/g) of the total surface area, while mesopores contributed 19.35% ( $100.94 \text{ m}^2/\text{g}$ ). The predominance of micropores allows the material to provide a large number of active channels, which facilitates the formation of multiple electric double layers, enhancing charge storage capacity. Consequently, the energy storage potential of the material is increased [34]. On the other hand, mesopores promote efficient, barrier-free ion transport, enabling fast migration throughout the electrode and access to all available sites, resulting in high power output [35]. The synergistic interaction of micropores and mesopores contributes to the excellent electrochemical performance of the material when used as an electrode [36]. The pore size distribution, as illustrated in Figure 5, further confirms the presence of various pore sizes. Micropores exhibit high adsorption in the 1.4-2.0 nm range, followed by sub-micropores in the 2.0-5.0 nm range. Mesopores, spanning 5-50 nm, are also well-defined, while macropores, though present in smaller quantities, were identified in the 51-200 nm range. Each pore size contributes positively to the material's electrochemical behaviour, enhancing the performance of energy storage devices.

To verify the presence of heteroatoms in the porous carbon material derived from acacia plantation residue, energy dispersive

spectroscopy (EDS) was conducted over a wide energy range of 0 to 20 keV, as shown in Figure 6. The EDS spectra revealed that carbon was the predominant element, constituting 91.73% of the material, confirming the successful conversion of acacia pods into high-purity carbon through the one-step integrated chemical-physical activation process. Additionally, significant amounts of heteroatom dopants were detected in the disrupted carbon chains. Oxygen, the second most abundant element, accounted for 7.07%, likely due to oxidation reactions filling the fractured carbon bonds [37]. Boron was detected at 1.06%, likely originating from the decomposition of specific proteins and minerals inherent in the biomass. Phosphorus, introduced through the catalytic agent H<sub>3</sub>PO<sub>4</sub>, was present in trace amounts (0.14%). The incorporation of these heteroatom dopants enhances the material's wettability, electrical conductivity, and mechanical/electrochemical stability, without adding excessive mass to the carbon structure [38]. Furthermore, the potential for Faradaic redox reactions associated with these dopants contributes to the material's pseudo-capacitive behaviour, synergistically enhancing its electrochemical double-layer capacitance (EDLC). This improved capacitive performance is further explored in the cyclic voltammetry and galvanostatic charge-discharge analyses of the acacia pod-derived carbon electrodes.

Self-doped porous carbon materials containing P, B, and O heteroatoms, derived from acacia plantation residues, were successfully synthesized and employed as working electrode materials for symmetric supercapacitors. The electrochemical performance of the electrodes was evaluated using standard method with CV dan GCD measurements. Symmetric electrodes were prepared in an H<sub>2</sub>SO<sub>4</sub> acidic electrolyte with a maximum operating voltage of 1 V. Initially, CV measurements were conducted at varying sweep rates, as depicted in Figure 7a. The hysteresis in the CV curves exhibited a distorted rectangular shape, characterized normal electric double-layer capacitors (EDLCs) [5,39]. Moreover, the presence of current spikes forming "camel hump" patterns indicated the occurrence of faradaic redox reactions due to the dopant species, suggesting pseudocapacitive behavior in the electrodes [40]. The combined effects of EDLC and pseudocapacitance synergistically enhanced the overall capacitance of the symmetric electrodes. Using standard equations, the specific capacitance of the electrode was calculated as 164 F/g at a scan rate of 1 mV/s and 112 F/g at 10 mV/s. Clearly, the specific capacitance decreased with increasing sweep rate, as shown in Figure 7b. This decline is attributed to reduced accessibility of active sites at higher sweep rates, limiting ion transport to the electrode's surface. Additionally, the contribution of faradaic reactions was analyzed using the Trasatti method, as illustrated in Figure 7c. The results showed that EDLC capacitance accounted for 67.06%, while pseudocapacitance contributed of 32.94%. This confirms that the incorporation of phosphorus, boron, and oxygen dopants significantly enhances the specific capacitance of porous carbon derived from acacia plantation residues [41].

The electrochemical behavior of this supercapacitor was further investigated through the analysis of GCD profiles at current densities ranging from 1 to 10 A/g, as shown in Figure 7d. Generally, the GCD curves exhibited a slightly asymmetric isosceles triangular shape, indicating good reversibility dominated by EDLC behavior. The asymmetry in the curves is attributed to faradaic

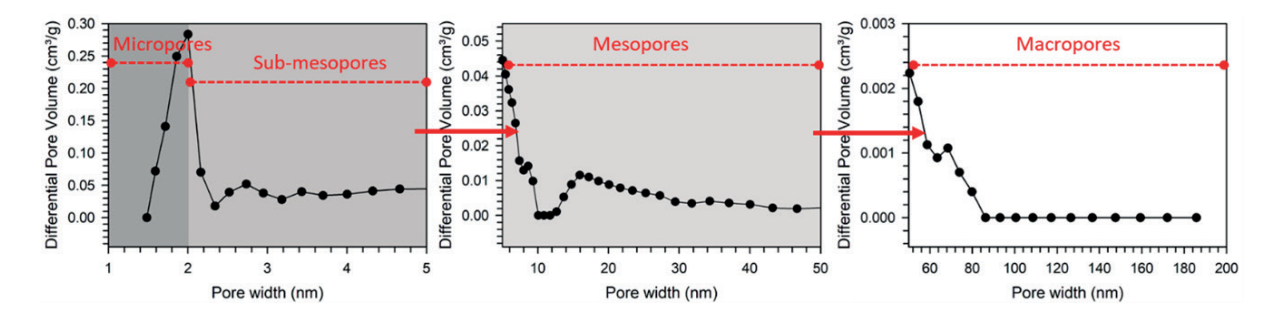


Figure 5. Pore size distribution of porous carbon

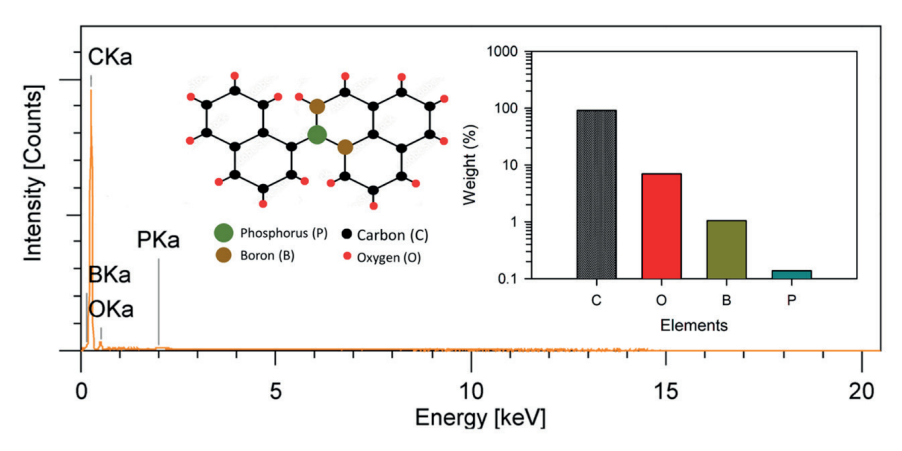


Figure 6. EDS spectra of porous carbon.

processes caused by the heteroatomic dopants—phosphorus, boron, and oxygen—suggesting the presence of pseudocapacitance. The faradaic redox reactions of phosphorus, boron, and oxygen in the  $H_2SO_4$  electrolyte on the electrode surface are detailed in Equations (1), (2), (3), and (4) [42,43]:

$$-P=O+2H^{+}+2e^{-} \rightleftharpoons -P(OH)$$
 (1)

$$*C-B-C=O + 2H^{+} + 2e^{-} \rightleftharpoons *C-B-CH(OH)$$
 (2)

$$-COO^{-} + H^{+} + e^{-} \rightleftharpoons -COOH \tag{3}$$

$$-C=O+H^{+}+e^{-} \rightleftharpoons -C-OH \tag{4}$$

These reactions allow for the diffusion of additional ions into the porous carbon, which is particularly beneficial at high current flow, promoting the formation of a stiff layer and an abundant Helmholtz region. This analysis confirms the synergistic EDLC-pseudocapacitance behavior previously observed in the CV results. Furthermore, at a current density of 1 A/g, the IR drop was negligible, and the material exhibited a coulombic efficiency of nearly 90%, reflecting its high conductivity. This high conductivity can be attributed to the successful design of the solid cylinder-like precursor, which required no additional external binders.

The specific capacitance of the electrode at 1 A/g was measured at 198 F/g. This enhancement is due to the synergistic effect of rich heteroatom doping combined with high specific surface area and a 3D-connected hierarchical pore structure. The carbon

material exhibited a specific surface area of 521 m<sup>2</sup>/g with a total pore volume of 0.293 cm<sup>3</sup>/g, where micropores accounted for 80.65% and mesopores for 19.35%. The dominance of micropores supports effective charge storage, while mesopores facilitate ion transport. This balanced pore structure contributes to the high specific capacitance of 198 F/g, demonstrating the crucial role of surface area and pore architecture in the electrochemical performance of the carbon-based supercapacitor. The capacitive properties of the electrode were also evaluated at various current densities, as illustrated in Figure 7e. While the specific capacitance decreased at higher current densities, the retention remained high, with 86.3% retention at 10 A/g. This is likely due to the mesopores, which comprise 19.35% of the total surface area, providing rapid ion insertion and extraction even at elevated current densities. Specifically, the capacitance values of the electrodes were 198, 156, 146, and 143 F/g at current densities of 1, 2, 5, and 10 A/g, respectively. Moreover, the energy and power outputs generated by the working electrode are represented through a Ragone plot, as shown in Figure 7f. The optimal energy output reached 14 Wh/ kg at a maximum power output of 670 W/kg. Compared to other previously studied heteroatom-doped symmetric supercapacitors [15,44], these results are highly competitive.

The potential for micro-scale applications of the assembled symmetric supercapacitors was also explored by examining their

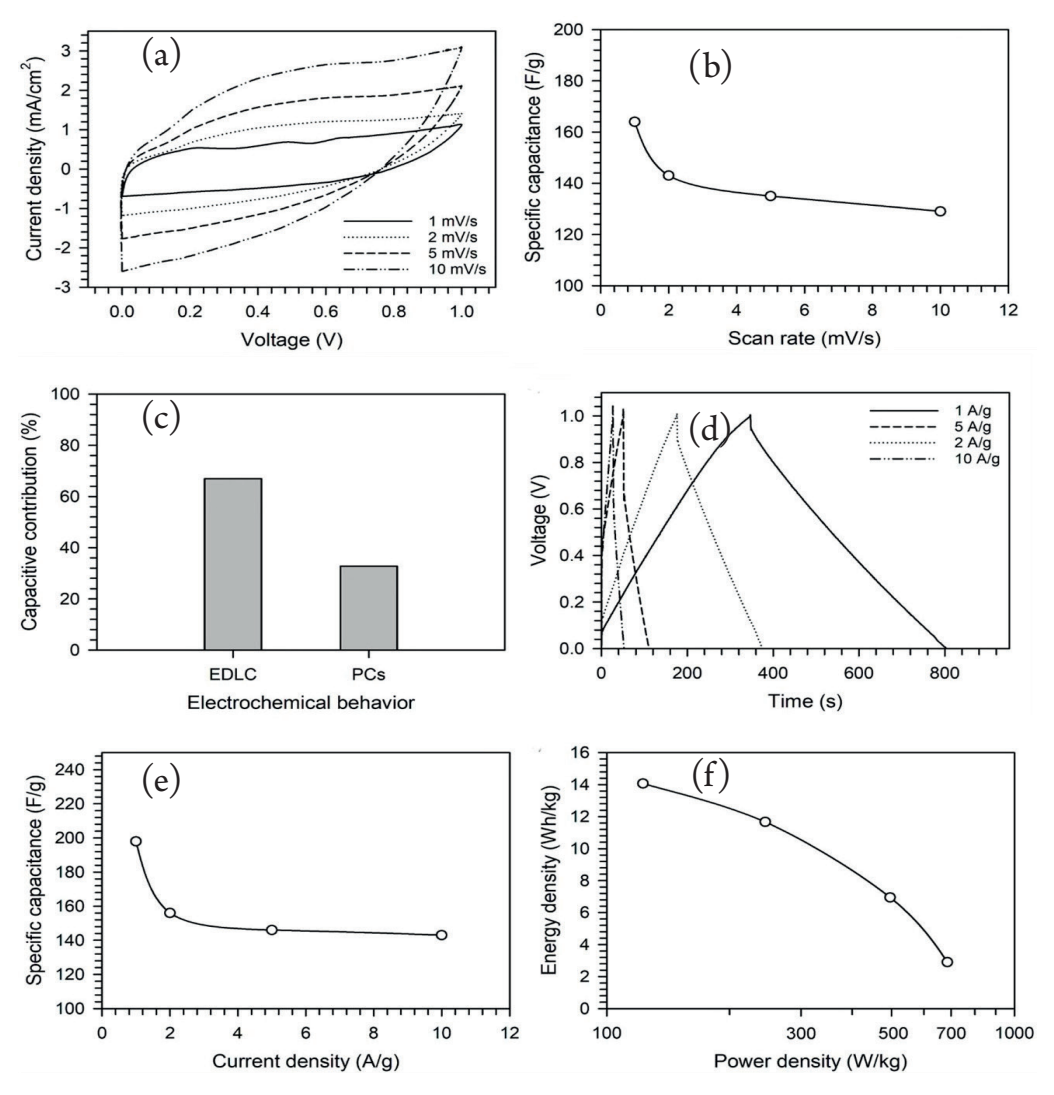


**Figure 7**. Schematic (a) CV profile in 1-10 mV/s, (b) specific capacitance vs. scan rate, (c) capacitive contribution, (d) GCD profile in 1-10 A/g, (e) specific capacitance vs. current density, and (f) Ragone plot.

**Table 1**. Comparison of electrochemical performance with different carbon sources.

Carbon sources	Morphology	Electrode	Impregnated	Csp (F/g)	E (Wh/kg)	P (Wh/kg)	Reff.
Melon peels	Hierarchical pores	2-E	$ZnCl_2$	158	29,5	830	[47]
sawdust	Hierarchical pores	3-E	КОН	80	11,12	252	[48]
Cassia fistula	sheet-like	2-E	КОН	136.5	7,2	3488.1	[49]
hemp fiber	coral-like	3-E	КОН	255.6	16.6	725	[50]
Bamboo	3D Pores	2-E	CH <sub>3</sub> COOK	236.35	8.21	62.5	[40]
Jack wood	Nanopores	2-E	NaOH	147	8.02	68.5	[15]
Marigold flower	Hierarchical pores	2-E	$ZnCl_2$	179	23	556	[51]
Acacia residue	Hierarchical pores	2-E	$H_3PO_4$	198	14	640	This study

volumetric capacitive performance. The dense electrode design, achieved without the use of external adhesives, resulted in a high density of 1.03 g/cm³, which is believed to contribute to the superior volumetric performance. Using standard calculations, the volumetric capacitance was measured at 203.4 F/cm³ at 1 A/g. Additionally, the volumetric energy and power outputs were evaluated, yielding values of 14.42 Wh/L and 690 W/L, respectively. These results surpass those reported in previous studies [45,46] utilizing different carbon sources (see Table 1). The findings and analyses presented here demonstrate that the porous carbon electrodes, self-doped with P, B, and O heteroatoms derived from acacia plantation residues, play a significant role in developing environmentally benign supercapacitors for sustainable energy storage applications.

# 4. CONCLUSION

In summary, acacia pods, a byproduct of acacia plantations, have been successfully converted into porous carbon self-doped P, B, and O heteroatoms, demonstrating potential for green supercapacitor applications. The one-step integrated chemical-physical activation process effectively transformed the precursor into a highly porous material with a 3D hierarchical structure connected by hexagonal pores. The carbon porosity, dominated by micropores (80.65%) and well-defined mesopores (19.35%), provides abundant active channels for rapid ion transport. The solid precursor design, free from external binders, resulted in a working electrode density of 1.03 g/cm<sup>3</sup>. Furthermore, the presence of phosphorus, boron, and oxygen heteroatoms was clearly detected, alongside high carbon content. The synergy of these material properties led to enhanced electrochemical performance, with a specific capacitance of 198 F/g at 1 A/g. Capacitance retention and coulombic efficiency were measured at 86% and 98%, respectively. The volumetric capacitance reached 203.4 F/cm<sup>3</sup>, while the energy and power outputs were 14 Wh/kg and 670 W/kg, respectively, in H2SO4 electrolyte media. Overall, the self-doped porous carbon containing P, B, and O heteroatoms demonstrates significant potential as an electrode material for enhancing the electrochemical performance of sustainable green supercapacitors.

# ACKNOWLEDGEMENTS

The authors would like to express their sincere gratitude to the Directorate of Research and Community Service, Republic of Indonesia for the financial support provided for this research, especially in Fundamental Research Scheme, grand contract: 102/C3/DT.05.00/PL/2025, derivative contract: 19521/UN19.5.1.3/AL.04/2025.

#### CREDIT AUTHOR STATEMENT

Apriwandi: Supervision, Conceptualization, Methodology, Writing-Original draft preparation, Writing-Reviewing and Editing. Rindhu Nabila Deniza: Investigation, Data curation, Formal analysis, Writing-Original draft preparation. Awaludin Martin: Visualization, Data curation, Formal analysis. Julnaidi Julnaidi: Data curation, Writing-Reviewing and Editing. Rika Taslim: Data curation, Formal analysis. Erman Taer: Conceptualization, Methodology.

# DECLARATIONS

**Conflict of interest** The authors declare that they have no known competing financial interests or personal relationships that could have appeared to influence the work reported in this paper.

### REFERENCES

- [1] Khan, H.A., Tawalbeh, M., Aljawrneh, B., Abuwatfa, W., Al-Othman, A., Sadeghifar, H., Olabi, A.G. A Comprehensive Review on Supercapacitors: Their Promise to Flexibility, High Temperature, Materials, Design, and Challenges. Energy 2024, 295, 131043, doi:10.1016/j.energy.2024.131043.
- [2] Hu, H., Yan, M., Jiang, J., Huang, A., Cai, S., Lan, L., Ye, K., Chen, D., Tang, K., Zuo, Q. A State-of-the-Art Review on Biomass-Derived Carbon Materials for Supercapacitor Applications: From Precursor Selection to Design Optimization. Sci. Total Environ. 2024, 912, 169141, doi:10.1016/j.scitotenv.2023.169141.
- [3] Sangtong, N., Chaisuwan, T., Wongkasemjit, S., Ishida, H.; Redpradit, W., Seneesrisakul, K., Thubsuang, U. Ultrahigh-Surface-Area Activated Biocarbon Based on Biomass Residue as a Supercapacitor Electrode Material: Tuning Pore Structure Using Alkalis with Different Atom Sizes. Microporous Mesoporous Mater. 2021, 326, 111383, doi:10.1016/j.micromeso.2021.111383.
- [4] Aruchamy, K., Dharmalingam, K., Lee, C.W., Mondal, D., Sanna Kotrappanavar, N. Creating Ultrahigh Surface Area Functional Carbon from Biomass for High Performance Supercapacitor and Facile Removal of Emerging Pollutants. Chem. Eng. J. 2022, 427, 131477, doi:10.1016/j. cej.2021.131477.
- [5] Taer, E., Yanti, N., Taslim, R., Apriwandi, A. Interconnected Micro-Mesoporous Carbon Nanofiber Derived from Lemongrass for High Symmetric Supercapacitor Performance. J. Mater. Res. Technol. 2022, 19, 4721–4732, doi:10.1016/j. jmrt.2022.06.167.
- [6] Taer, E., Febriyanti, F., Mustika, W.S., Taslim, R., Agustino, A., Apriwandi, A. Enhancing the Performance of Supercapacitor Electrode from Chemical Activation of Carbon Nanofibers Derived Areca Catechu Husk via One-Stage Integrated Pyrolysis. Carbon Lett. 2021, 31, 601–612, doi:10.1007/s42823-020-00191-5.
- [7] Chakraborty, R., Sharma, A., Maji, P.K., Rudra, S., Kumar, A., Nath, P., Naik, Y., Pradhan, M. Nitrogen and Oxygen Self-Doped Hierarchical Porous Carbon Nanosheets Derived from Turmeric Leaves for High-Performance Supercapacitor. Inorganica Chim. Acta 2024, 567, 122056, doi:10.1016/j.ica.2024.122056.
- [8] Xue, C. F., Lin, Y., Zhao, W., Wu, T., Wei, Y. Y., Li, X. H., Yan, W. J., Hao, X.G. Green Preparation of High Active Biochar with Tetra-Heteroatom Self-Doped Surface for Aqueous Electrochemical Supercapacitor with Boosted Energy Density. J. Energy Storage 2024, 90, 111872, doi:10.1016/j.est.2024.111872.
- [9] H. Julnaidi, Saputra, E., Nofrizal, Taer, E. Renewable Palm Oil Sticks Biomass-derived Unique Hierarchical Porous Carbon

- Nanostructure as Sustainability Electrode for Symmetrical Supercapacitor. J. Chem. Technol. Biotechnol. 2023, 98, 45–56, doi:10.1002/jctb.7217.
- [10] Kavan Kumar, V., Panwar, N. L. A Review on Porous Carbon Synthesis Processes and Its Application as Energy Storage Supercapacitor. J. Indian Chem. Soc. 2024, 101, 101231, doi:10.1016/j.jics.2024.101231.
- [11] Taer, E., Natalia, K., Apriwandi, A., Taslim, R., Agustino, A., Farma, R. The Synthesis of Activated Carbon Nano Fiber Electrode Made from Acacia Leaves (Acacia Mangium Wild) as Supercapacitors. Adv. Nat. Sci. Nanosci. Nanotechnol. 2020, 11, 25007, doi:10.1088/2043-6254/ab8b60.
- [12] Wang, Q., Zheng, H., Zhang, Y., Huang, Y., Li, W., Huang, W., Xiang, J., Yuan, P., Xue, H., Wang, S. Biomass-Based Porous Carbon from Trachycarpus Fortunei Silk with the Hierarchical Oxygen-Enriched Structure for High Performance Flexible All-Solid-State Supercapacitor. J. Phys. Chem. Solids 2024, 185, 111785, doi:10.1016/j.jpcs.2023.111785.
- [13] Anand, S., Wasi Ahmad, M., Syed, A., Bahkali, A.H., Verma, M., Hye Kim, B., Choudhury, A. Walnut Shell Derived N, S Co-Doped Activated Carbon for Solid-State Symmetry Supercapacitor Device. J. Ind. Eng. Chem. 2024, 129, 309–320, doi:10.1016/j.jiec.2023.08.045.
- [14] Xu, H., Dong, L., Zhang, B., Wang, K., Meng, J., Tong, Y., Wang, H. Heteroatom Self-Doped Graphitic Carbon Materials from Sargassum Thunbergii with Improved Supercapacitance Performance. Adv. Sens. Energy Mater. 2024, 100102, doi:10.1016/j.asems.2024.100102.
- [15] Bandara, T. M. W., Alahakoon, A. M. B., Mellander, B., E., Albinsson, I. Activated Carbon Synthesized from Jack Wood Biochar for High Performing Biomass Derived Composite Double Layer Supercapacitors. Carbon Trends 2024, 15, 100359, doi:10.1016/j.cartre.2024.100359.
- [16] Peng, S., Lu, S., Wang, X., Dai, L., Chen, B., Wu, Y., Xie, Q., Ruan, Y. Hierarchical Rapeseed Stalk-Derived Activated Carbon Porous Structure with N and O Codoping for Symmetric Supercapacitor. Colloids Surfaces A Physicochem. Eng. Asp. 2024, 688, 133666, doi:10.1016/j.colsurfa.2024.133666.
- [17] Nor, N.S.M., Deraman, M., Omar, R., Taer, E., Awitdrus, Farma, R., Basri, N.H., Dolah, B.N.M. Nanoporous Separators for Supercapacitor Using Activated Carbon Monolith Electrode from Oil Palm Empty Fruit Bunches. AIP Conf. Proc. 2014, 1586, 68–73, doi:10.1063/1.4866732.
- [18] Chen, Z., Chen, Y., Wang, Q., Yang, T., Luo, Q., Gu, K., Yang, W. Molecularly-Regulating Oxygen-Containing Functional Groups of Ramie Activated Carbon for High-Performance Supercapacitors. J. Colloid Interface Sci. 2024, 665, 772–779, doi:10.1016/j.jcis.2024.03.177.
- [19] Sun, R., Chen, Y., Gao, X., Xie, G., Yang, R., Yang, C., Shi, Y., Yi, Y. Sodium Lignosulfonate-Derived Hierarchical Porous Carbon Electrode Materials for Supercapacitor Applications. J. Energy Storage 2024, 91, 112025, doi:10.1016/j.est.2024.112025.
- [20] Apriwandi, A., Taer, E., Farma, R., Setiadi, R.N., Amiruddin, E. A Facile Approach of Micro-Mesopores Structure Binder-Free Coin/Monolith Solid Design Activated Carbon for Electrode Supercapacitor. J. Energy Storage 2021, 40, 102823, doi:10.1016/j.est.2021.102823.

- [21] Sarwar, A., Ali, M., Khoja, A.H., Nawar, A., Waqas, A., Liaquat, R., Naqvi, S.R., Asjid, M. Enhancing the Performance of Supercapacitor Electrode from Chemical Activation of Carbon Nanofibers Derived Areca Catechu Husk via One-Stage Integrated Pyrolysis. J. CO2 Util. 2021, 46, 101476, doi:10.1016/j.jcou.2021.101476.
- [22] Zhao, Y., Mu, J., Wang, Y., Liu, Y., Wang, H., Song, H. Preparation of Hierarchical Porous Carbon through One-Step KOH Activation of Coconut Shell Biomass for High-Performance Supercapacitor. J. Mater. Sci. Mater. Electron. 2023, 34, 1–22, doi:10.1007/s10854-023-09885-8.
- [23] Oginni, O., Singh, K., Oporto, G., Dawson-Andoh, B., Mc-Donald, L., Sabolsky, E. Effect of One-Step and Two-Step H3PO4 Activation on Activated Carbon Characteristics. Bioresour. Technol. Reports 2019, 8, 100307, doi:10.1016/j. biteb.2019.100307.
- [24] Li, Y., Zhang, X., Yang, R., Li, G., Hu, C. The Role of H3PO4 in the Preparation of Activated Carbon from NaOH-Treated Rice Husk Residue. RSC Adv. 2015, 5, 32626–32636, doi:10.1039/c5ra04634c.
- [25] Tobi, A.R., Dennis, J.O. Activated Carbon from Composite of Palm Bio-Waste as Electrode Material for Solid-State Electric Double Layer Capacitor. J. Energy Storage 2021, 42, 103087, doi:10.1016/j.est.2021.103087.
- [26] Deraman, M., Daik, R., Soltaninejad, S., Nor, N.S.M.; Awitdrus; Farma, R.; Mamat, N.F.; Basri, N.H.; Othman, M.A.R. A New Empirical Equation for Estimating Specific Surface Area of Supercapacitor Carbon Electrode from X-Ray Diffraction. Adv. Mater. Res. 2015, 1108, 1–7, doi:10.4028/www.scientific.net/AMR.1108.1.
- [27] Nframah Ampong, D., Lin, W., de Souza, F.M., Kishore Bharti, V., Ofori Agyemang, F., Andrews, A., Mensah-Darkwa, K., Dhakal, A., Mishra, S.R., Perez, F., et al. Utilization of Shea Butter Waste-Derived Hierarchical Activated Carbon for High-Performance Supercapacitor Applications. Bioresour. Technol. 2024, 406, 131039, doi:10.1016/j.biortech.2024.131039.
- [28] Mary, A.J.C., Nandhini, C., Bose, A.C. Hierarchical Porous Structured N-Doped Activated Carbon Derived from Helianthus Annuus Seed as a Cathode Material for Hybrid Supercapacitor Device. Mater. Lett. 2019, 256, 126617, doi:10.1016/j.matlet.2019.126617.
- [29] Taer, E., Pratiwi, L., Apriwandi, Mustika, W.S., Taslim, R., Agustino Three-Dimensional Pore Structure of Activated Carbon Monolithic Derived from Hierarchically Bamboo Stem for Supercapacitor Application. Commun. Sci. Technol. 2020, 5, 22–30, doi:10.21924/cst.5.1.2020.180.
- [30] A. Taer, E., Apriwandi, A., Nursyafni, N., Taslim, R. Averrhoa Bilimbi Leaves-Derived Oxygen Doped 3D-Linked Hierarchical Porous Carbon as High-Quality Electrode Material for Symmetric Supercapacitor. J. Energy Storage 2022, 52, 104911, doi:10.1016/j.est.2022.104911.
- [31] Sanglaow, T., Prasert, K., Chanthad, C., Liangruksa, M., Sutthibutpong, T. A DFT Study on the Fundamental Mechanisms of Quantum Capacitance Enhancement within the Carbon-Based Electrodes through Different Classes of Doped Configurations from Biomass-Derived Elements. Results Mater. 2024, 21, 100529, doi:10.1016/j.rinma.2024.100529.

- [32] Víctor G. Baldovino-Medranoa, V.N.-C., Isaacs-Giraldo, R. Systematic Analysis of the Nitrogen Adsorption-Desorption Isotherms Recorded for a Series of Microporous Mesoporous Amorphous Aluminosilicates Using Classical Methods Víctor G. Baldovino-Medrano. 2020.
- [33] H.W. Wen, Z., Wang, Q., Yang, Y., Si, L. Pore Structure Characteristics and Evolution Law of Different-Rank Coal Samples. Geofluids 2021, 2021, 1–17, doi:10.1155/2021/1505306.
- [34] Yao, Y., Yu, Y., Ge, D., Zhang, Y., Du, C., Ye, H., Wan, L., Chen, J., Xie, M. Nanocarbon of Moderate Microporosity Doped with Oxygenate Redox Pairs to Achieve Superior Gravimetic/Volumetric Supercapacitor Performances. Appl. Surf. Sci. 2023, 612, 155811, doi:10.1016/j.apsusc.2022.155811.
- [35] Qin, Q., Wang, J., Tang, Z., Jiang, Y., Wang, L. Mesoporous Activated Carbon for Supercapacitors Derived from Coconut Fiber by Combining H3PO4-Assisted Hydrothermal Pretreatment with KOH Activation. Ind. Crops Prod. 2024, 208, 117878, doi:10.1016/j.indcrop.2023.117878.
- [36] Taer, E., Apriwandi, A., Febriani, W., Taslim, R. Suitable Micro/Mesoporous Carbon Derived from Galangal Leaves (Alpinia Galanga L.) Biomass for Enhancing Symmetric Electrochemical Double-Layer Capacitor Performances. ChemistrySelect 2022, 7, e202201810, doi:10.1002/slct.202201810.
- [37] Ghosh, S., Barg, S., Jeong, S.M., Ostrikov, K. Heteroatom-Doped and Oxygen-Functionalized Nanocarbons for High-Performance Supercapacitors. Adv. Energy Mater. 2020, 10, 1-44, doi:10.1002/aenm.202001239.
- [38] Gopalakrishnan, A., Badhulika, S. Effect of Self-Doped Heteroatoms on the Performance of Biomass-Derived Carbon for Supercapacitor Applications. J. Power Sources 2020, 480, 228830, doi:10.1016/j.jpowsour.2020.228830.
- [39] Taer, E., Handayani, R., Apriwandi, A., Taslim, R., Awitdrus; Amri, A., Agustino, Iwantono, I. The Synthesis of Bridging Carbon Particles with Carbon Nanotubes from Areca Catechu Husk Waste as Supercapacitor Electrodes. Int. J. Electrochem. Sci. 2019, 14, 9436–9448, doi:10.20964/2019.10.34.
- [40] Yue, W., Yu, Z., Zhang, X., Liu, H., He, T., Ma, X. Green Activation Method and Natural N/O/S Co-Doped Strategy to Prepare Biomass-Derived Graded Porous Carbon for Supercapacitors. J. Anal. Appl. Pyrolysis 2024, 178, 106409, doi:10.1016/j.jaap.2024.106409.
- [41] Ma, Y., Zhang, X., Liang, Z., Wang, C., Sui, Y. B/P/N/O Co-Doped Hierarchical Porous Carbon Nanofiber Self-Standing Film with High Volumetric and Gravimetric Capacitance Performances for Aqueous Supercapacitors. Electrochim. Acta 2020, 337, 135800, doi:10.1016/j.electacta.2020.135800.
- [42] A. Kong, S., Xiang, X., Jin, B., Guo, X., Wang, H., Zhang, G., Huang, H., Cheng, K. B, O and N Codoped Biomass-Derived Hierarchical Porous Carbon for High-Performance Electrochemical Energy Storage. Nanomaterials 2022, 12, 1720, doi:10.3390/nano12101720.
- [43] Chen, B., Wu, W., Li, C., Wang, Y., Zhang, Y., Fu, L., Zhu, Y., Zhang, L., Wu, Y. Oxygen/Phosphorus Co-Doped Porous Carbon from Cicada Slough as High-Performance Electrode Material for Supercapacitors. Sci. Rep. 2019, 9, 1–8, doi:10.1038/s41598-019-41769-y.
- [44] Yang, Yang, Q., Guo, J., Zhang, S., Wang, W., Zhang, X., He,

- J., Xu, Y. Utilizing Waste Pomelo Peel to Develop Activated-Doped Porous Biomass Carbon as Electrode Materials: Study of Activation Mechanism, Evaluation of Electrochemical Properties and Assembly of Symmetric Supercapacitors. Ind. Crops Prod. 2024, 209, 118060, doi:10.1016/j.indcrop.2024.118060.
- [45] P. Zhang, S., Yu, Y., Xie, M., Du, C., Chen, J., Wan, L., Zhang, Y. Clean Production of N, O-Doped Activated Carbon by Water Vapor Carbonization/Activation of Expired Coffee for High-Volumetric Supercapacitor. Appl. Surf. Sci. 2022, 589, 153011, doi:10.1016/j.apsusc.2022.153011.
- [46] Yang, M., Zeng, X., Zhang, X., Yang, Z. 3D Silk Fibroin/ Carbon Nanotube Array Composite Matrix for Flexible Solid-State Supercapacitors. New J. Chem. 2020, 44, 6575– 6582, doi:10.1039/d0nj00351d.
- [47] Ahmad, N., Rinaldi, A., Sidoli, M., Magnani, G., Vezzoni, V., Scaravonati, S., Pasetti, L., Fornasini, L., Gupta, H.; Tamagnone, M.; et al. Pre-Treated Biomass Waste Melon Peels for High Energy Density Semi Solid-State Supercapacitors. J. Power Sources 2024, 624, doi:10.1016/j.jpowsour.2024.235511.
- [48] Tafete, G.A., Uysal, A., Habtu, N.G., Abera, M.K., Yemata, T.A., Duba, K.S., Kinayyigit, S. Hydrothermally Synthesized Nitrogen-Doped Hydrochar from Sawdust Biomass for Supercapacitor Electrodes. Int. J. Electrochem. Sci. 2024, 19, doi:10.1016/j.ijoes.2024.100827.
- [49] Rajivgandhi, P., Mariappan, A., Manivannan, M., Kumar Dharman, R., Hwan Oh, T., Sekar, A. Biomass Waste Derived from Cassia Fistula into Value-Added Porous Carbon Electrode for Aqueous Symmetric Supercapacitors. Inorg. Chem. Commun. 2024, 165, 1–7, doi:10.1016/j.inoche.2024.112552.
- [50] Gao, Y., Liu, C., Jiang, Y., Zhang, Y., Wei, Y., Zhao, G., Liu, R., Liu, Y., Shi, G., Wang, G. Hydrothermal Assisting Biomass into a Porous Active Carbon for High-Performance Supercapacitors. Diam. Relat. Mater. 2024, 148, doi:10.1016/j.diamond.2024.111487.
- [51] Jangra, R., Mahendia, P., Karakoti, M., Sahoo, N.G., Srivastava, A., Sinha, O.P., Clemons, T.D., Deshpande, U., Mahendia, S. ZnCl2-Assisted Conversion of Nitrogen-Containing Biomass Carbon from Marigold Flower: Toward Highly Porous Activated Nitrogen-Doped Carbon for Low ESR and Enhanced Energy Density Supercapacitors. J. Energy Storage 2024, 75, 109728, doi:10.1016/j.est.2023.109728.